

# **Hydrogen Peroxide / Kerosene, Liquid-Oxygen / Kerosene, and Liquid-Oxygen / Liquid Methane for Upper Stage Propulsion**

S. Krishnan\*

Universiti Teknologi Malaysia, Skudai 81310, Malaysia

## **ABSTRACT**

A study engine of 85kN and 700s for upper stage propulsion is considered to compare the stage performance of three bipropellant combinations: 1) hydrogen peroxide (H<sub>2</sub>O<sub>2</sub>) - kerosene (RP1), 2) liquid oxygen (LOX) - RP1, and 3) LOX - liquid methane (LCH<sub>4</sub>). Recent interests in H<sub>2</sub>O<sub>2</sub> as well as LCH<sub>4</sub> have motivated this study. Theoretical rocket-engine performance values are presented for the three propellant combinations. On reviewing the available industrial data of upper stages using these propellants, the stage-mass estimations are presented. Results indicate that the oxidizer fuel ratio adopted by industry for upper stage engines of LOX-RP1 or LOX-LCH<sub>4</sub> are higher than that corresponding to the maximum specific impulse calculated under frozen flow assumption. Stage performance results demonstrate that the H<sub>2</sub>O<sub>2</sub>-RP1 stage with its highest density specific impulse has the heaviest stage mass of 115 percent, but the lowest stage volume by 77 percent. However, its attainable velocity increment is expected to be slightly higher than that of LOX-RP1 stage and about the same with respect to that of LOX-LCH<sub>4</sub> stage.

### *Keywords:*

Upper stage propulsion, Hydrogen peroxide, Stage performance

## **Nomenclature**

$F$	thrust
$I$	total impulse
$I_s$	specific impulse
$m_s$	stage empty-mass without payload
$m_p$	total-propellant mass
$p_c$	chamber pressure
$p_e$	nozzle exit plane pressure
$T_0$	adiabatic flame temperature

### *Greek Symbols*

$\alpha$	mass concentration of hydrogen peroxide
$\varepsilon$	nozzle area-ratio
$\eta_c^*$	$c^*$ combustion efficiency
$\eta_{I_s}$	specific-impulse efficiency

---

\* Address for correspondence: Department of Aeronautical Engineering, Faculty of Mechanical Engineering, Universiti Teknologi Malaysia, 81310 Skudai, Malaysia. Tel.: +60 7 5534650; fax: +60 7 5576820.

E-mail address: subramaniamkrishnan@hotmail.com

$\rho_p$	propellant density
$\Phi$	oxidizer-fuel ratio
$\varphi$	equivalence ratio

### *Subscripts*

$e$	equilibrium flow assumption
$f$	frozen flow assumption
$max$	maximum condition
$vac$	vacuum operation

## 1. Introduction

Liquid oxygen (LOX) and kerosene (RP1) bipropellant systems are widely adopted for application in first and upper-stage propulsion. In recent years, however, there has been a renewed interest in the use of hydrogen peroxide ( $H_2O_2$ ) as an oxidizer for upper stage propulsion. Although numerous studies have been reported in the last two decades on the use of  $H_2O_2$ -RP1 as a propellant combination, some recent ones are Sisco et al. (2005), Cong et al. (2004), Tan et al. (2009), Wernimont and Durant (2004), Miller et al. (2003), and Ventura and Mullens (1999). On many accounts,  $H_2O_2$  is considered to be a well suited “green” propellant. Rocket-grade  $H_2O_2$  (concentration  $\alpha \geq 0.85$ ) is a non-toxic monopropellant as well as an oxidizer. It is of high density with a high optimum oxidizer-fuel-ratio, which will enable the realization of a compact propulsion-system. A propulsion unit without a requirement for a separate ignition unit offers higher system-reliability.  $H_2O_2$  decomposes into an environmental-friendly mixture of superheated steam and oxygen at a temperature in excess of 1000K. This leads to an automatic ignition either with a liquid fuel in a bipropellant engine or with a solid fuel in a hybrid-rocket engine. Its low vapor pressure at room temperature facilitates easy and safe ground-handling. Ventura et al. (2007) present an interesting discussion to refute several misconceptions about  $H_2O_2$  on its stability and storage, detonation sensitivity, catalyst-bed longevity, space applications, and chemical toxicity, and establish that it is a well-suited propellant for various propulsion and power applications.

Currently, on a different aspect, the cryogenic-fuel liquid-methane (LCH<sub>4</sub>) is of interest for upper stage applications. LCH<sub>4</sub> was proposed as a propellant by the Russians as early as 1980’s. Because of the possibility of harvesting oxygen and methane on lunar and Martian soils, there have been related research activities in developing propulsion systems that use the combination of LOX-LCH<sub>4</sub> for interplanetary missions (Melcher and Allred, 2009; Barsi et al., 2008). In parallel, industries in many countries are actively developing LOX-LCH<sub>4</sub> engines for upper stage applications — for example see the annual reviews on liquid propulsion (Anon., 2008; Anon., 2009). This interest in employing LCH<sub>4</sub> for upper stage application is due to its higher density, as well as the relative ease in handling and storing of this propellant when compared to liquid hydrogen. Furthermore, in recent years, lower operational and developmental costs are becoming more important than the need to realize higher specific impulse for space propulsion.

In consideration of the aspects discussed previously, the present study analyzes and compares the upper-stage performance-figures of the three propellants:  $H_2O_2$ -RP1, LOX-RP1, and LOX-LCH<sub>4</sub>. For the comparative study, one can start with a chosen orbital change and

arrive at the optimal minimum velocity increment ( $\Delta v^*$ ) through a trajectory optimization. For this  $\Delta v^*$ , the comparative study can be carried out among possible propellant combinations to choose the best combination and the related engine configuration. Such a comparison will be specific to the chosen orbital change. For the present study, alternatively, without fixing a particular orbital change we choose the specification of an upper stage engine that has served multiple launch-functions. Results of such a comparative study are expected to be more general in nature. The upper stage engine RD58M is the one which has rendered diverse launch functions: low earth-orbit, medium earth-orbit, geosynchronous transfer orbit, and also transvenusian, and transmartian ones. The technical details of this engine are as follows. Application in stages: Proton 11S824M, 11S824F, 11S86, 11S861, and 17S40 (all of 4<sup>th</sup> and final stage); gross stage mass range: 17550 – 14000 kg; payload range: 6220 – 1880 kg; propellants: LOX-RP1; rated vacuum thrust: 83.4 kN; vacuum specific impulse: 3462 N-s/kg ; applied burn time range: 450 - 610 s (design nominal: 680s); engine mass: 230 kg; chamber pressure: 7.75 MPa; nozzle area ratio: 189; oxidizer-fuel ratio: 2.48; country of origin: Russia; status: in production; first flight: 1974; last flight: 2006; flown: 212 times (Encyclopedia Astronautica, <http://www.astronautix.com>). In consideration of this versatile engine, the specifications of the engine chosen for the comparative study are: vacuum thrust = 85kN, burn time = 700s, nozzle area-ratio = 190, and chamber pressure = 8 MPa.

The objective of the study is not to recommend the best propellant combination but to present the stage performance data for the three propellant combinations though simple but reasonably detailed calculations. The results of the study could possibly prompt further elaborate comparative-analysis.

## 2. Calculations

The properties of the propellants are listed in Table 1. The theoretical performance prediction procedures for rocket engines can be very advanced, adopting chemical non-equilibrium modeling with relevant computational fluid dynamic codes from combustion chamber to nozzle exit (Miller and Barrington, 1970). However, in line with the objective of the study as previously stated, a one dimensional procedure has been followed using the program CEC71 (Gordon and McBride, 1971). Both equilibrium and frozen flow assumptions are considered; the concentration  $\alpha$  of H<sub>2</sub>O<sub>2</sub> is taken as 0.98.

Mass distribution of the stage without payload for each of the three propellant combinations is calculated based on the current technology values. Theoretical velocity increments in a gravity free vacuum with zero payloads are calculated to compare the performance of the stages.

**Table 1**  
Properties of propellants.

Property	LOX	H <sub>2</sub> O <sub>2</sub>	RP1 (CH <sub>1.9423</sub> )	LCH4
Density (kg/m <sup>3</sup> )	1149	1443	773	421
Freezing point (°C)	-219	1	-73	-184
Boiling point (°C)	-183	150	147	-162
Specification	MIL-P-25508	MIL-H-16005	MIL-R-25576	-
Heat of formation (kJ/kg)	-405.6	-5520.3	-1626.8	-5562.5

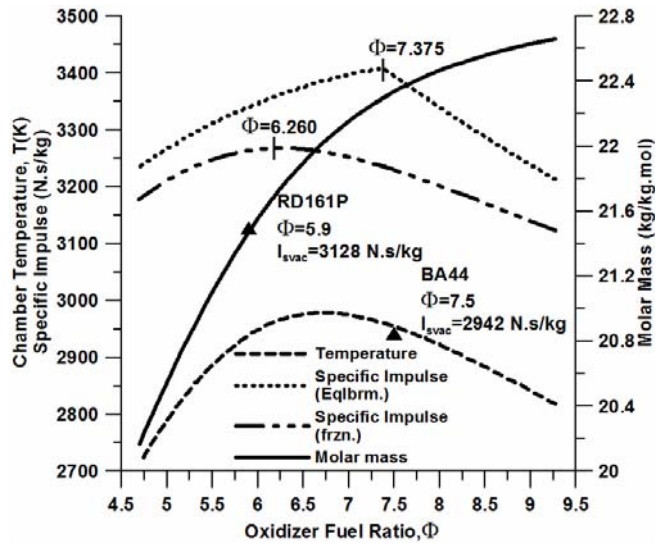


Figure 1 Theoretical rocket performance of  $\text{H}_2\text{O}_2$ -RP1 propellant combination.  $\text{H}_2\text{O}_2$  concentration = 0.98, chamber pressure = 8 MPa, and nozzle area ratio = 190.

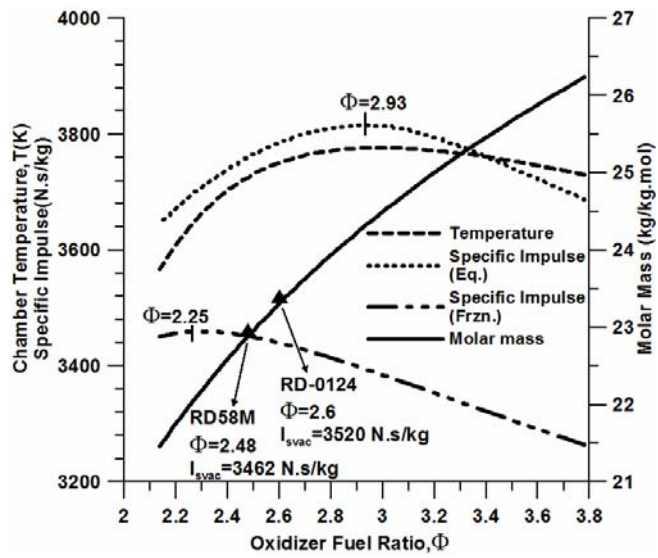


Figure 2 Theoretical rocket performance of LOX-RP1 propellant combination. Chamber prssure = 8 MPa and nozzle area ratio = 190.

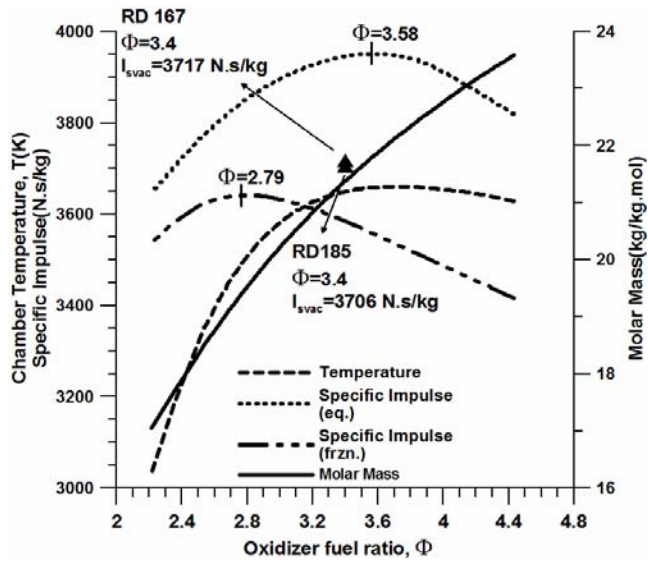


Figure 3 Theoretical rocket performance of LOX-LCH<sub>4</sub> propellant combination. Chamber pressure = 8 MPa and nozzle area ratio = 190.

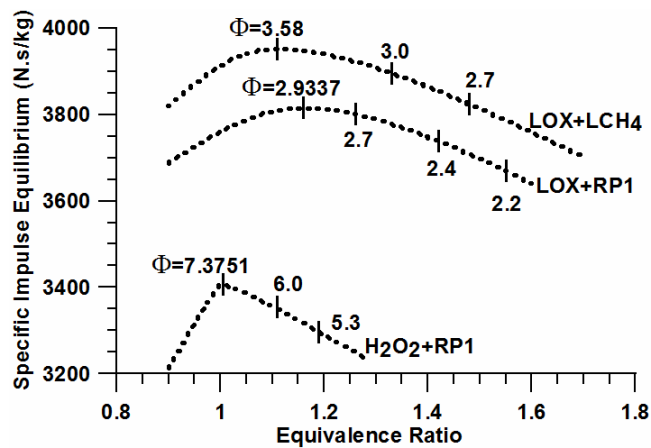


Figure 4 Comparison of shifting equilibrium specific impulse of three propellant combinations: H<sub>2</sub>O<sub>2</sub>-RP1, LOX-RP1, and LOX-LCH<sub>4</sub>. Chamber pressure = 8 MPa and nozzle area ratio = 190.

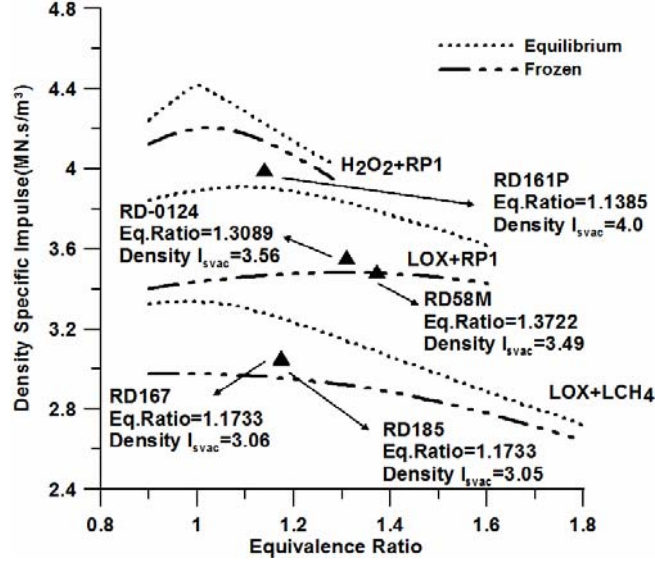


Figure 5 Comparison of density specific impulse for H<sub>2</sub>O<sub>2</sub>-RP1, LOX-RP1, and LOX-LCH<sub>4</sub> propulsion systems. Chamber pressure = 8 MPa and nozzle area ratio = 190.

### 3. Results and Discussion

The calculated results of the theoretical rocket performance are given in Figs. 1-3. The specific impulse and density specific impulse comparisons for the three propellant combinations are shown in Figs. 4 and 5. A summary of these results are given in Table 2. As numerous performance figures are given in this table, a brief clarification of the numbers is in order. There are six columns of numbers with two columns for each propellant combination. As an example, let us consider the first two columns of numbers corresponding to equilibrium and frozen flow calculations for H<sub>2</sub>O<sub>2</sub>-RP1. All numbers without square brackets in the first column of numbers correspond to the condition of maximum equilibrium specific impulse ( $I_{s_e}$ )<sub>max</sub>, shown as the column heading. Additionally, all numbers within the square brackets in this column refer to the condition of maximum density specific impulse calculated under equilibrium flow assumption ( $\rho_p I_{s_e}$ )<sub>max</sub>, shown as the column heading within the square brackets. Similarly, corresponding to the frozen flow calculations, the numbers of the next column without and with square brackets relate to the conditions of maximum specific impulse ( $I_{s_f}$ )<sub>max</sub> and maximum density specific impulse ( $\rho_p I_{s_f}$ )<sub>max</sub> respectively. In the case of H<sub>2</sub>O<sub>2</sub>-RP1 propellant combination, under equilibrium flow assumption, maximum specific impulse as well as maximum density specific impulse occurs at the equivalence ratio of 1. As usual, for the LOX-RP1 and LOX-LCH<sub>4</sub> the maximum specific impulse values are reached at the fuel rich conditions.

As expected, from the results of the analysis (Figs. 1 - 5 and Table 2), the highest specific impulse occurs for the LOX-LCH<sub>4</sub>, but its density specific impulse is the lowest. Having a high density specific impulse, rather than a high specific impulse, is an important point for the selection of propellant combination in volume limited systems. On this point the H<sub>2</sub>O<sub>2</sub>-RP1 with its highest density specific impulse is expected to be a candidate. As stated previously, here we

consider the stage to be independent, that is, the stage without payload. The major part of the stage burnout-mass, or the stage-empty mass  $m_s$ , is the mass of propellant tanks and feed system. The balance consists of the engine itself, which forms about 10 percent of  $m_s$ . The choice of H<sub>2</sub>O<sub>2</sub>, with its high density and high optimum oxidizer-fuel ratio  $\Phi$  values for its combination with RP1, is expected to give the least volume of the total propellant to be handled. As the propellant volume to be handled reduces, the mass of the propellant tanks and the feed system — and in turn the stage burnout mass  $m_s$  — is also reduced.

### 3.1. *Industrial data*

The available data for sample upper stage engines, which use the three propellant combinations, and which closely resemble the study engine, are given in Table 3 (Encyclopedia Astronautica, <http://www.astronautix.com>; Ventura and Garboden, 1999). As explained previously for Table 2, the numbers without and within the square brackets correspond to the respective headings. Although engines which utilize the propellant combination H<sub>2</sub>O<sub>2</sub>-RP1 are reportedly being currently developed, the tabulated examples are from those of limited availability in open literature, either flown but out of production (Gamma-2 of 1969-'71), or of design study (RD161P, BA-44 and BA-810 of the 1990's). The adopted concentration of H<sub>2</sub>O<sub>2</sub>, if known for the sample engine, is given in Table 3. The listed LOX-RP1 engines have flown many times, until recently. The LOX-LCH<sub>4</sub> engines are in development, or at the design study phase. As only nozzle pressure ratios ( $p_c/p_e$ 's) are known for the LOX-LCH<sub>4</sub> engines RD-185 and RD-167, the calculated nozzle area ratio corresponding to frozen flow (the one of lower value) as well as that corresponding to equilibrium flow is listed.

The nominal  $\Phi$  value adopted for an engine of a particular propellant combination depends on the optimum conditions of specific impulse and density specific impulse, the design and its application, and the additives added to base propellants. Although the  $\Phi$  values adopted by the industries for the H<sub>2</sub>O<sub>2</sub>-RP1 engines of the past do not lead to any conclusion, Fig. 1, it is seen that the adopted values of  $\Phi$  for LOX-RP1 and LOX-LCH<sub>4</sub> engines tend to be higher than the ones of optimum specific impulse of frozen flow assumption, Figs. 2 and 3. Such a choice for the H<sub>2</sub>O<sub>2</sub>-RP1 engines, currently under development, is expected to result in the highest effect on system compactness because of the high density of H<sub>2</sub>O<sub>2</sub> and the inherently high optimum  $\Phi$  values.

**Table 2**

Summary of the values of theoretical performance for the propellant combinations H<sub>2</sub>O<sub>2</sub>-RP1, LOX-RP1, and LOX-LCH<sub>4</sub>.

	H <sub>2</sub> O <sub>2</sub> -RP1		LOX-RP1		LOX-LCH <sub>4</sub>	
	at $(I_{s_e})_{max}$ & [ $(\rho_p I_{s_e})_{max}$ ]	at $(I_{s_f})_{max}$ & [ $(\rho_p I_{s_f})_{max}$ ]	at $(I_{s_e})_{max}$ & [ $(\rho_p I_{s_e})_{max}$ ]	at $(I_{s_f})_{max}$ & [ $(\rho_p I_{s_f})_{max}$ ]	at $(I_{s_e})_{max}$ & [ $(\rho_p I_{s_e})_{max}$ ]	at $(I_{s_f})_{max}$ & [ $(\rho_p I_{s_f})_{max}$ ]
$I_{s_e}$ (N-s/kg)	3407 [3407]	3363 [3396]	3815 [3808]	3709 [3789]	3951 [3906]	3850 [3861]
$I_{s_f}$ (N-s/kg)	3236 [3236]	3268 [3254]	3395 [3370]	3460 [3438]	3557 [3482]	3642 [3447]
$\rho_p I_{s_e}$ (MN-s/m <sup>3</sup> )	4.422 [4.422]	4.304 [4.386]	3.901 [3.910]	3.714 [3.837]	3.295 [3.339]	3.038 [3.336]
$\rho_p I_{s_f}$ (MN-s/m <sup>3</sup> )	4.200 [4.200]	4.182 [4.203]	3.471 [3.461]	3.465 [3.482]	2.967 [2.977]	2.873 [2.978]
$\Phi$	7.38 [7.38]	6.26 [6.96]	2.93 [3.09]	2.30 [2.62]	3.58 [4.03]	2.79 [4.24]
$\varphi$	1.00 [1.00]	1.18 [1.06]	1.16 [1.10]	1.48 [1.30]	1.12 [0.99]	1.43 [0.94]
$T_0$ (K)	2961 [2961]	2967 [2976]	3776 [3776]	3663 [3753]	3659 [3653]	3503 [3642]

**Table 3**

Data of sample upper stage engines.

Propellants	Engine name	$F_{vac}$ (kN) [ $p_c$ (bar)]	$\Phi$ [ $\eta_{I_s}$ ]	$I_{s_{vac}}$ (N-s/kg) [ $\varepsilon$ ]	$I$ (kN-s) [ $m_s/m_p$ ]
H <sub>2</sub> O <sub>2</sub> (~0.97)-RP1	RD161P <sup>b</sup>	24.5 to 14.7 [117.7]	5.9 [0.93]	3128 [265]	17640 [--]
H <sub>2</sub> O <sub>2</sub> (~0.83)-RP1	Gamma-2 <sup>a,d</sup>	68.2 [31]	8.23 [--]	2599 [--]	7707 [0.18]
H <sub>2</sub> O <sub>2</sub> (--)-RP1	BA-44 <sup>b,e</sup>	196 to 98 [--]	7.5 [--]	2941 [100]	88200 [0.08]
H <sub>2</sub> O <sub>2</sub> (--)-RP1	BA-810 <sup>b,e</sup>	3600 to 1800 [--]	7.5 [--]	2765 [25]	453600 [0.08]
LOX-RP1	S1-5400A <sup>a</sup>	67.3 [54.0]	-- [--]	3354 [--]	13460 [0.210]
LOX-RP1	RD-58M <sup>a,d</sup>	83.4 [77.5]	2.48 [0.92]	3462 [189]	56712 [0.15]
LOX-RP1	RD-0124 <sup>a,d</sup>	294.3 [162]	2.60 [--]	3520 [--]	88290 [0.103]
LOX-LCH <sub>4</sub>	RD-185 <sup>b</sup>	179 [147.0]	3.4 [0.93]	3706 [188- 260] $p_c/p_e = 4167$	-- [--]
LOX-LCH <sub>4</sub>	RD-167 <sup>c,d</sup>	353 [167.0]	3.4 [0.94]	3717 [162-220] $p_c/p_e = 3400$	-- [--]

<sup>a</sup>Flown. <sup>b</sup>Development. <sup>c</sup>Design concept. <sup>d</sup>Pump fed. <sup>e</sup>Pressure fed.

The specific impulse efficiency  $\eta_{I_s}$  is defined as the ratio of the vacuum specific impulse reported by the industry and that calculated for equilibrium flow assumption. Specific impulse losses are due to incomplete combustion, heat transfer, friction, and divergence and non-equilibrium flow in the nozzle. In general  $\eta_{I_s}$  is found to be in the range of 0.90 to 0.94, and the higher values generally correspond to recently developed engines. The values of  $\eta_{I_s}$  for some engines, if they can be calculated from the available data, are given in Table 3. Regarding H<sub>2</sub>O<sub>2</sub>-RP1 engines presented in Table 3, RD161P is the development engine of the 1990's. It used a high concentration of H<sub>2</sub>O<sub>2</sub> ( $\alpha = 0.96$  to 0.98), and its  $\eta_{I_s}$  is close to 0.93. Gamma-2 is a flight proven second stage engine of late 1960's and it used a relatively low concentration H<sub>2</sub>O<sub>2</sub> ( $\alpha = 0.80$  to 0.85). However, its nozzle area ratio is not known. Additionally, the values of  $\alpha$  adopted in BA-44 and BA-810 are not known. Therefore,  $\eta_{I_s}$  values for these three engines could not be calculated.

### 3.2. Performance estimation of study stages

As the available data on  $\eta_{I_s}$  for H<sub>2</sub>O<sub>2</sub>-RP1 engines are old and scant, we have to arrive at a suitable value of  $\eta_{I_s}$  for the H<sub>2</sub>O<sub>2</sub>-RP1 study engine in order to derive the possible experimental specific-impulse. In the normal course, the complete reaction of H<sub>2</sub>O<sub>2</sub>-RP1 is engineered in two stages — first by the decomposition of H<sub>2</sub>O<sub>2</sub> in a suitable catalyst pack, and subsequently by the combustion of decomposed H<sub>2</sub>O<sub>2</sub> with RP1. In order to circumvent this two-stage process, there are at present attempts to induce a hypergolic condition between H<sub>2</sub>O<sub>2</sub> and RP1 with the use of suitable additives (Cong et al., 2004), and to develop H<sub>2</sub>O<sub>2</sub>-RP1 torch igniters that will enable direct combustion between injected H<sub>2</sub>O<sub>2</sub> and RP1 (Fisher, 2002). Recent studies on H<sub>2</sub>O<sub>2</sub>-RP1 thrusters indicate a  $c^*$  combustion efficiency  $\eta_c^*$  in the range of 0.92 – 0.94 (Wernimont and Durant, 2004; Miller et al., 2003). These values of  $\eta_c^*$  are typical of most other liquid-propellant combinations. Notwithstanding the technology improvement that has taken place over the years, and considering the handicap due to the possible adoption of the two-stage reaction-process, it appears conservative to assume a value of 0.90 as the  $\eta_{I_s}$  for H<sub>2</sub>O<sub>2</sub>-RP1 upper stage engines.

The data on  $\Phi$  values being adopted are not available for the current H<sub>2</sub>O<sub>2</sub>-RP1 engines under development. The values of  $\Phi$  adopted for the H<sub>2</sub>O<sub>2</sub>-RP1 engines of the past are 5.9 at  $\alpha = 0.97$  average concentration for RD161P, 8.23 at  $\alpha = 0.83$  average concentration for Gamma-2, and 7.5 of unknown concentration for BA-44, Table 3. The calculations of the present study at  $\alpha = 0.98$  indicate the maximum equilibrium flow specific impulse  $(I_{s_e})_{max}$  as well as maximum equilibrium density specific impulse  $(\rho_p I_{s_e})_{max}$  at  $\Phi = 7.38$ ; maximum frozen flow specific impulse  $(I_{s_f})_{max}$  at  $\Phi = 6.26$ ; and maximum frozen flow density specific impulse  $(\rho_p I_{s_f})_{max}$  at  $\Phi = 6.96$ , Table 2 and Fig. 5. As the engines of LOX-RP1 and LOX-LCH<sub>4</sub> employ values of  $\Phi$  greater than the ones corresponding to  $(I_{s_f})_{max}$ , we have considered for the H<sub>2</sub>O<sub>2</sub>-RP1 study engine two values of  $\Phi$ , one at 7.38 and the other at 6.96, which correspond to  $(\rho_p I_{s_e})_{max}$  and  $(\rho_p I_{s_f})_{max}$  respectively. As discussed previously, the corresponding equilibrium flow specific impulse is multiplied by the  $\eta_{I_s} = 0.90$  to arrive at the estimated experimental specific impulse for H<sub>2</sub>O<sub>2</sub>-RP1 combination, Tables 2 and 4. For the LOX-RP1 combination, the  $\Phi$  value of 2.48 of the reference engine RD 58M is taken for the stage calculations. For the LOX-LCH<sub>4</sub> combination, both the sample engines use  $\Phi$  value of 3.4, and the same is adopted. For the study engines of LOX-RP1 and LOX-LCH<sub>4</sub>, the realizable values of experimental specific impulse are calculated by adopting  $\eta_{I_s} = 0.93$  and 0.94 respectively, Tables 3 and 4. After allowing 2.5 percent for valve passages and piping, the total propellant mass is calculated. We allowed 5 percent for ullage in our calculations of total propellant tank volumes. As the total propellant tank volume forms a major part of the stage volume, this is taken as the value to represent the relative stage volume, Table 4.

For a chosen propellant combination, generally the  $m_s/m_p$  fraction reduces as the total propellant volume to be handled increases. The study engine uses H<sub>2</sub>O<sub>2</sub> concentration  $\alpha$  of 0.98 and is of 85kN thrust for 700 s. This results in a total impulse of 59500 kN-s with a total propellant tank volume of about 16.2 m<sup>3</sup>, Table 4. The pump-fed flight-proven Gamma-2 engine,

using an H<sub>2</sub>O<sub>2</sub>-concentration  $\alpha = 0.83$  average, was of 68.2 kN thrust for 113s — that amounts to a total impulse of 7707 kN-s. Its stage Black Arrow - 2 had an  $m_s/m_p$  of 0.18. The pressure-fed development-engine BA-44, using an unknown concentration of H<sub>2</sub>O<sub>2</sub>, was of 147 kN average thrust for 600s, and that amounts to a total impulse of 88200 kN-s. Its stage Beal BA-2 Stage 3 had an  $m_s/m_p = 0.084$ .

**Table 4.**

Stage performance of H<sub>2</sub>O<sub>2</sub>-RP1, LOX-RP1, and LOX-LCH4.

	<b>H2O2-RP1</b>		<b>LOX-RP1</b>	<b>LOX-LCH4</b>
Oxidizer fuel ratio adopted by industry [assumed for H <sub>2</sub> O <sub>2</sub> -RP1]	7.38	6.96	2.48	3.4
Specific impulse realized by industry [estimated assuming $\eta_{I_s} = 0.9$ for H <sub>2</sub> O <sub>2</sub> -RP1] (N-s/kg)	3066	3057	3463	3691
Total propellant mass, $m_p$ (kg)	19888	19953	17611	16526
Total-propellant tank volume (m <sup>3</sup> ) (Relative stage volume)	16.09	16.22 (1)	18.34 (1.13)	21.04 (1.30)
(Assumed $m_s/m_p$ )	(0.085 – 0.1)	(0.085 – 0.1)	(0.15)	(0.15)
Stage empty mass, $m_s$ (kg)	1691 – 1989	1696 – 1995	2642	2479
Stage gross mass (kg) (Relative stage mass)	21579 – 21877	21649 – 21948 (1)	20253 (0.93)	19004 (0.87)
Velocity increment in zero-gravity vacuum with zero payload (km/s) (Relative velocity increment)	7.81 – 7.35	7.78 – 7.33 (1)	7.05 (0.93)	7.52 (1)

As the available  $m_s/m_p$  values of the H<sub>2</sub>O<sub>2</sub>-RP1 stages are from the past and consist of limited data, in order to adopt a suitable value of  $m_s/m_p$  for the H<sub>2</sub>O<sub>2</sub>-RP1 study stage, we can look for the stage performance values of a similar propellant combination. The earth storable nitrogen tetroxide and unsymmetrical dimethyl hydrazine (N<sub>2</sub>O<sub>4</sub>-UDMH) is one such combination. Average propellant density for the H<sub>2</sub>O<sub>2</sub>-RP1 is 1295 kg/m<sup>3</sup> while that for the N<sub>2</sub>O<sub>4</sub>-UDMH is 1180 kg/m<sup>3</sup>. The adopted  $\Phi$  for N<sub>2</sub>O<sub>4</sub>-UDMH is around 2.6, while that for H<sub>2</sub>O<sub>2</sub>-RP1 is about 7.2. The specific impulse values are more or less the same. In effect, for similar stages with more or less of an equal propellant mass  $m_p$ , the propellant volume of N<sub>2</sub>O<sub>4</sub>-UDMH is expected to be more than that of H<sub>2</sub>O<sub>2</sub>-RP1 and hence the  $m_s/m_p$  (a fraction largely dependent on the total propellant volume for the given  $m_p$ ) is expected to be more for N<sub>2</sub>O<sub>4</sub>-UDMH than for H<sub>2</sub>O<sub>2</sub>-RP1. With the N<sub>2</sub>O<sub>4</sub>-UDMH, the stage UR700-4 with the engine 11D423 having a total propellant volume of about 26.5 m<sup>3</sup> had an  $m_s/m_p$  fraction of 0.06. With the same combination, the stage 8K94 with the engine RD857 having a total propellant volume

of about  $8.3 \text{ m}^3$  had an  $m_s/m_p$  fraction of 0.10. Therefore, it is reasonable and conservative to assume a value of 0.085 to 0.1 for  $m_s/m_p$  for the H<sub>2</sub>O<sub>2</sub>-RP1 study stage. Thus the calculated stage empty mass  $m_s$  is in the range of 1696 to 1995 kg, Table 4.

The  $m_s$  for the LOX-RP1 study stage is estimated from the PROTON 11S861 stage that adopted the engine RD-58M, which closely resembles the study engine. The stage PROTON 11S861 had a propellant volume of about  $14.7 \text{ m}^3$  and had an  $m_s/m_p$  fraction of 0.155. The study stage of LOX-RP1 has a propellant volume of  $17.47 \text{ m}^3$ . Therefore assuming  $m_s/m_p = 0.15$ , the empty mass for the LOX-RP1 study stage is calculated as 2642 kg, Table 4. For the LOX-LCH<sub>4</sub> study stage, having an enhanced propellant volume of  $20.03 \text{ m}^3$  with reduced propellant mass and having both its propellants as cryogenic,  $m_s/m_p$  is expected to be more than 0.15. Nevertheless, assuming the same value of  $m_s/m_p = 0.15$ , the empty mass for the LOX-LCH<sub>4</sub> study stage is calculated to be 2479 kg, Table 4.

The calculated results, with a conservative value of  $\eta_{I_s} = 0.9$  given in Table 4, indicate that the H<sub>2</sub>O<sub>2</sub>-RP1 study stage has the lowest stage volume by 77 percent but the heaviest stage mass of 115 percent. However, its attainable velocity increment in gravity free vacuum with zero payload is expected to be 7 percent higher than that of LOX-RP1 stage, and about the same with respect to that of LOX-LCH<sub>4</sub> stage. These comparative values are given for  $\Phi = 6.96$  for H<sub>2</sub>O<sub>2</sub>-RP1. If we take  $\Phi = 7.38$  (a six percent increase in its operating  $\Phi$  from 6.96), it does not bring appreciable improvement in the performance. On the other hand, if we assume a 2 percent improvement in specific impulse efficiency ( $\eta_{I_s} = 0.92$ ), a substantial improvement of the same order in the stage performance of H<sub>2</sub>O<sub>2</sub>-RP1 is seen.

#### 4. Conclusions

Choosing a particular engine specification for upper stage application, the present study calculated the theoretical rocket performance of three propellant combinations: hydrogen peroxide and kerosene, liquid oxygen and kerosene, and liquid oxygen and liquid methane. Furthermore, from the available industrial data, the upper stage performances for the three propellant combinations were determined. For the conservatively assumed specific impulse efficiency of 0.90 for the hydrogen peroxide and kerosene stage, its velocity increment in gravity free vacuum with zero payload is slightly more than that of the liquid oxygen and kerosene stage, and comparable to that of the liquid oxygen and liquid methane stage. As expected, the hydrogen peroxide and kerosene stage is the most compact but the heaviest. While the performance of this stage is insensitive to the variation of oxidizer-fuel ratio, the effect due to the improvement in specific impulse efficiency on stage is substantial. Considering the environmentally friendly characteristics of hydrogen peroxide and the substantially reduced developmental and operational cost of the earth storable hydrogen peroxide and kerosene propellant combination, further detailed comparative study of this propellant combination for upper stage application appears to be of importance.

#### Acknowledgements

The present study forms a part of the research supported by the Ministry of Science Technology and Innovation of Malaysia. Muhammad Idris Bin Sazali, a senior undergraduate student of the Faculty, drafted the figures presented here.

## References

- Anon., (2008) Liquid Propulsion, *Aerospace America*, 46 (12), pp. 66-67.
- Anon., (2009) Liquid Propulsion, *Aerospace America*, 47 (12), p. 38.
- Barsi, S. Moder, J. and Kassemi, M., (2008) Numerical Investigation of LO<sub>2</sub> and LCH<sub>4</sub> Storage Tanks on the Lunar Surface, 44<sup>th</sup> AIAA/ASME/SAE/ASEE Joint Propulsion Conference and Exhibit, AIAA 2008-4749.
- Cong, Y. Zhang, T. Li, T. Sun, J. Wang, X. Ma, L. Liang, D. and Lin, L., (2004) Propulsive Performance of a Hypergolic H<sub>2</sub>O<sub>2</sub>/Kerosene Bipropellant, *J. Propulsion and Power*, 20 (1), pp. 83-86.
- Encyclopedia Astronautica, Retrieved June 28, 2010, from <http://www.astronautix.com>.
- Fisher, S.C., (2002) Liquid Propulsion, *Aerospace America*, 40 (12), pp. 64-65.
- Gordon, S. and McBride, B.J. (1971) Computer Program for Calculation of Complex Chemical Equilibrium Compositions, Rocket Performance, Incident and Reflected Shocks, and Chapman-Jouguet Detonations, NASA SP-273.
- Melcher IV, J.C. and Allred, J.K., (2009) Liquid Oxygen / Liquid Methane Test Results of the RS-18 Lunar Ascent Engine at Simulated Altitude Conditions at NASA White Sands Test Facility, 45<sup>th</sup> AIAA/ASME/SAE/ASEE Joint Propulsion Conference and Exhibit, AIAA 2009-4949.
- Miller, K. Sisco, J. Austin, B. Martin, T. and Anderson, W., (2003) Design and Ground Testing of a Hydrogen Peroxide / Kerosene Combustor for RBCC Application, 39<sup>th</sup> AIAA/ASME/SAE/ASEE Joint Propulsion Conference and Exhibit, AIAA 2003-4477.
- Miller, W.H. and Barrington, D.K., (1970) A Review of Contemporary Solid Rocket Motor Performance Prediction Techniques, *J. Spacecraft and Rockets*, 7 (3), pp. 225-237.
- Sisco, J.C. Austin, B.L. Mok, J.S. and Anderson, W. E., (2005) Autoignition of Kerosene by Decomposed Hydrogen Peroxide in a Dump-Combustor Configurations, *J. Propulsion and Power*, 21 (3), pp.450-459.
- Tan, J. Liu, J. Yang, T. and Wang, Z., (2009) On Shut-off Explosion of High Test Hydrogen Peroxide/RP-1 Engine, 45<sup>th</sup> AIAA/ASME/SAE/ASEE Joint Propulsion Conference and Exhibit, AIAA 2009-4849.
- Ventura, M. and Garboden, G., (1999) A Brief History of Concentrated Hydrogen Peroxide Uses, 35<sup>th</sup> AIAA/ASME/SAE/ASEE Joint Propulsion Conference and Exhibit, AIAA99-31435.
- Ventura, M. and Mullens, P., (1999) The Use of Hydrogen Peroxide for Propulsion and Power, 35<sup>th</sup> AIAA/ASME/SAE/ASEE Joint Propulsion Conference and Exhibit, AIAA 99-2880.
- Ventura, M. Wernimont, E. Heister, S. and Yuan, S., (2007) Rocket Grade Hydrogen Peroxide (RGHP) for Use in Propulsion and Power Devices – Historical Discussion of Hazards, 43<sup>rd</sup> AIAA/ASME/SAE/ASEE Joint Propulsion Conference and Exhibit, AIAA 2007-5468.
- Wernimont, E. and Durant, D., (2004) Development of a 250 lbfv Kerosene – 90% Hydrogen Peroxide Thruster, 40<sup>th</sup> AIAA/ASME/SAE/ASEE Joint Propulsion Conference and Exhibit, AIAA 2004-4148.